Surface Science 633 (2015) 24–28

Contents lists available at ScienceDirect

Surface Science

journal homepage: www.elsevier.com/locate/susc

Effect of hydrogen adsorption on the electronic and optical properties of the Mg-doped O-terminated ZnO surface

Mohammed Ali Lahmer [a,*], Kamel Guergouri [b]

[a] Physics Department, University of Boumerdes, Boumerdes 35000, Algeria
[b] Physics Department, Larbi Ben M'Hidi University, University of Oum El Bouaghi, Oum El Bouaghi 04000, Algeria

ARTICLE INFO

Article history:
Received 13 September 2014
Accepted 14 November 2014
Available online 22 November 2014

Keywords:
ZnO
Hydrogen
Adsorption
First principles
Polar surface

ABSTRACT

The effect of hydrogen adsorption on the electronic structures and optical properties of undoped and Mg-doped ZnO $\left(000\bar{1}\right)$ polar surface was investigated using the first principles method. The obtained results show that hydrogen adsorption is more favored on Mg doped-ZnO $\left(000\bar{1}\right)$ surface than onto the clean surface, and this makes Mg-doped ZnO and $Mg_xZn_{1-x}O$ more efficient for H storage or gas sensing applications than undoped ZnO. On the other hand, our results show that the hydrogen adsorption on the Mg doped surface is energetically very preferable when the surface was prepared under O-rich conditions. We have also examined the effect of H adsorption on the optical properties of the surface.

1. Introduction

Zinc oxide (ZnO) is a wide-band-gap semiconductor with a band gap of 3.3 eV at room temperature. This material has recently attracted much attention because of potential applications in optoelectronic and transparent devices [1,2]. Among the proposed applications, the ZnO gas sensors are believed to be the most promising due to their low cost, low power consumption, high response, and rapid recovery. Recently, many theoretical and experimental works have focused on the high performance of ZnO based gas sensors employed in detecting a range of gases, such as H_2, Cl_2, CO, H_2O, H_2S, NO_2, SO_2, NH_3, CO_2, methane, and acetone [3–25].

Mg atom is an important element for the realization of ZnO-based optoelectronic devices and solar cells [26]. Mg doping may modulate the value of the ZnO band gap by the formation of ternary alloy $Mg_xZn_{(1-x)}O$ [27,28]. On the other side, surface segregation of Mg can lead to enhanced and stable green emission of ZnO nanoparticle [29].

In this paper, we use density-functional theory (DFT) to investigate the surface relaxation and the adsorption of atomic hydrogen atom onto clean and Mg-doped O-terminated ZnO $\left(000\bar{1}\right)$ polar surface. The adsorption geometries and the adsorption energies of the hydrogen atom adsorbed on different sites of ZnO surface are obtained. We are also interested to investigate the effect of hydrogen adsorption on the optical properties of undoped and Mg-doped ZnO $\left(000\bar{1}\right)$ surface.

2. Computational details

All calculations are performed by using the first-principles pseudopotential method based on density functional theory (DFT) within local density approximation (LDA) and generalized gradient approximation (GGA) as implemented in the Siesta package [30,31]. The pseudopotentials are constructed by the Troullier–Martins scheme [32]. The Ceperley–Alder exchange-correlation functional, as parametrized by Perdew and Zunger [33], is employed for LDA calculations. The obtained results are verified using the GGA–PBE exchange-correlation functional [34]. In our calculations, the double-ζ plus polarization basis sets are chosen for Zn, O and Mg respectively and the double-ζ basis set is used for H. For the bottom slab terminated surface atoms, pseudo H atoms with single-ζ basis set are used to saturate the dangling bonds. A real space mesh cut-off of 350 Ry and a reciprocal space grid cut-off of approximately 15 Å were used. The structure relaxation was done using the conjugated gradient method until the Hellman–Feynman force on each atom is smaller than 0.05 eV/Å.

For the study of H adsorption on a ZnO $\left(000\bar{1}\right)$ surface, we employ a slab model with a 2×2 surface unit cell consisting of five Zn–O bilayers and a vacuum layer of 12 Å separating the slabs (Fig. 1). The top three Zn–O bilayers as well as the adatom layer are allowed to relax while the bottom two bilayers of ZnO are fixed at their bulk positions to mimic the bulk substrate. The dangling bonds at the bottom layer are saturated using pseudo-hydrogen atoms with a nuclear charge of 1.5*e* in order to prevent unphysical charge transfer between the top and bottom slab surfaces. The use of pseudo-hydrogen atoms with a nuclear charge of 1.5*e* rather than the usual H atoms can be explained as next; in

* Corresponding author. Tel.: +213 024816249.
E-mail address: malahmer@yahoo.fr (M.A. Lahmer).

http://dx.doi.org/10.1016/j.susc.2014.11.014
0039-6028/

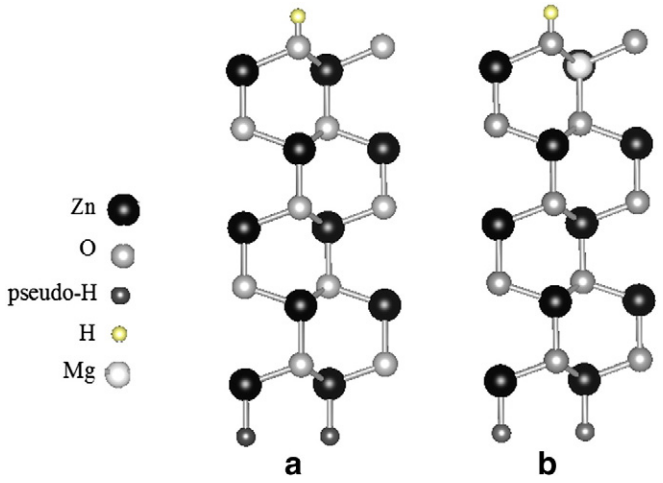

Fig. 1. Side view of the O-terminated ZnO $\left(000\bar{1}\right)$ polar surface configuration model used in this study, a) perfect surface, b) Mg-doped ZnO $\left(000\bar{1}\right)$ surface with H atom on top site.

the perfect w–ZnO bulk structure each atom is surrounded by four nearest-neighbor atoms, however, at the polar ZnO surfaces one of the four nearest-neighbor bonds of the surface atoms is broken. Since O contributes six and Zn two electrons to the four covalent bonds (covalent model), partially occupied dangling bonds will appear at the surfaces with 3/2 and 1/2 electrons per surface atom at the O- and Zn-terminated surface, respectively, forming a 3/4 and a 1/4 filled surface band. To passivate the bottom surface which is a Zn-terminated surface we use pseudo-hydrogen atoms with a 1.5*e* nuclear charge. The optimized bond length between a saturating pseudoatom and the Zn back side atoms is 1.73 Å [35].

The Gamma centered grids of $(4 \times 4 \times 1)$ *k* points were used for the Brillouin zone integration. The Mg-doping was done by replacing one of the Zn atoms in the first Zn surface layer with an Mg atom (Fig. 1b).

The thermodynamic stability of a given surface is determined by its surface energy γ, which can be calculated by the following formula:

$$\gamma = \frac{(E_{Slab} - NE_{Bulk})}{A} \tag{1}$$

where E_{Slab} is the total energy of the ZnO slab, E_{Bulk} is the total energy of bulk ZnO unit cell (with two oxygen and two zinc atoms), N is the number of ZnO unit cells in the slab model, and A is the surface area.

The adsorption energy for different surface configurations (different H coverages) was calculated according to

$$E_a = E_{slab+nH} - E_{slab} - n_H\mu_H \tag{2}$$

while in the case of Mg-doped ZnO $\left(000\bar{1}\right)$ surface:

$$E_a = E_{slab+nH}(ZnO+Mg) - E_{slab}(ZnO) - n_H\mu_H - n_{Mg}\mu_{Mg} + n_{Zn}\mu_{Zn} \tag{3}$$

where $E_{slab+nH}$ is the total energy of the undoped and Mg-doped ZnO $\left(000\bar{1}\right)$ slab with n_H adsorbed hydrogen atoms. E_{slab} is the total energy of the clean ZnO$\left(000\bar{1}\right)$ slab. μ_H, μ_{Zn} and μ_{Mg} are the chemical potentials of H, Zn and Mg respectively.

The chemical potential of oxygen is restricted within the thermodynamically allowed ranges determined by the corresponding formation enthalpy of bulk ZnO (ΔH^f_{ZnO}) and gas phase of O ($\mu^{gas}_{O_2}$).

The allowed range for the chemical potential $\Delta\mu_O$ is given by:

$$\Delta H^f_{ZnO} \leq \Delta\mu_O \leq 0. \tag{4}$$

The surface energy depends on the chemical potential of Zn and O atoms (μ_{Zn} and μ_O), and this dependence can be simplified by eliminating μ_O in favor of μ_{Zn} using the bulk thermodynamic equilibrium condition:

$$\Delta\mu_{Zn} + \Delta\mu_O = \Delta H^f_{ZnO} \tag{5}$$

which give the allowed range for Zn chemical potential:

$$\mu^{Bulk}_{Zn} + \Delta H^f_{ZnO} \leq \mu_{Zn} \leq \mu^{Bulk}_{Zn} \tag{6}$$

where μ^{Bulk}_{Zn} is chemical potential of Zn in the hcp structure $\left(\mu^{Bulk}_{Zn} = \frac{1}{2}E_{Zn}(hcp)\right)$.

The Mg chemical potential is calculated according to:

$$\mu_{Mg} = \frac{1}{2}E_{Mg}(hcp) \tag{7}$$

where $E_{Mg}(hcp)$ is the total energy of the hcp structure.

3. Results and discussion

Before studying the effect of hydrogen adsorption on the properties of the Mg-doped ZnO $\left(000\bar{1}\right)$ surface, we first consider the clean and the Mg-doped ZnO $\left(000\bar{1}\right)$ surface. The calculated lattice constants of $a = 3.226$ Å and $c = 5.219$ Å are obtained for wurtzite ZnO which give a Zn–O bond lengths of 1.9706 Å and 1.966 Å for bond direction perpendicular and parallel to the c axis respectively. For clean ZnO $\left(000\bar{1}\right)$ surface, the Zn–O bond lengths of 1.89 Å and 2.02 Å for bond direction perpendicular and parallel to the c axis are obtained for the first double layer which means that the O-terminated ZnO polar surface tends to relax inward, in good agreement with the previous results [36]. After Mg doping, the structure relaxation around the Mg_{Zn} atom becomes more important and the Mg–O bond lengths of 1.88 Å and 1.97 Å for bond direction perpendicular and parallel to the c axis are obtained.

In Table 1 we have summarized the H adsorption energies onto clean and Mg-doped ZnO $\left(000\bar{1}\right)$ surface as obtained from this work using both LDA and GGA methods. We can show that both LDA and GGA energies are in agreement within 0.5 eV. On the other side, the two methods suggest that the structure with 1/2 ML H coverage is the most stable surface under H-rich conditions, in very good agreement with the previous results [12]. Since LDA and GGA give us the same conclusions we will limit our discussion in most cases to LDA results only.

Fig. 2 shows the calculated adsorption energies for adsorbed atomic hydrogen on top site of the ZnO $\left(000\bar{1}\right)$ surface under different coverage conditions for both clean and Mg-doped ZnO $\left(000\bar{1}\right)$ surface respectively. These results show that at H-rich conditions the structure with a 1/2 ML H coverage is the most stable structure. Firstly, we compare the obtained results for H adsorption on the clean ZnO $\left(000\bar{1}\right)$ surface with available results in the literature in particular the results of Meyer [12]. The calculated hydrogen adsorption energies obtained in this work appear to be slightly different from the published results and this can be attributed to differences in the used computational methods. We note also that in Ref [12] the author has an interest to the change in the surface energy $\Delta\gamma$ of the ZnO $\left(000\bar{1}\right)$ surface under hydrogen adsorption coverage while in our work we focus on calculating the adsorption energy, however, there is a direct relation between

Table 1
The LDA and PBE H adsorption energies E_a (eV) as obtained for clean and Mg-doped ZnO $\left(000\bar{1}\right)$ surfaces with different H coverage (C_H).

C_H	Clean surface		Mg-doped surface	
	LDA	PBE	LDA	PBE
1/4	−2.20	−2.06	−5.38	−4.70
1/2	−4.23	−3.73	−7.48	−6.99
3/4	−3.91	−3.23	−7.05	−6.87
1	−2.95	−2.13	−6.02	−6.08

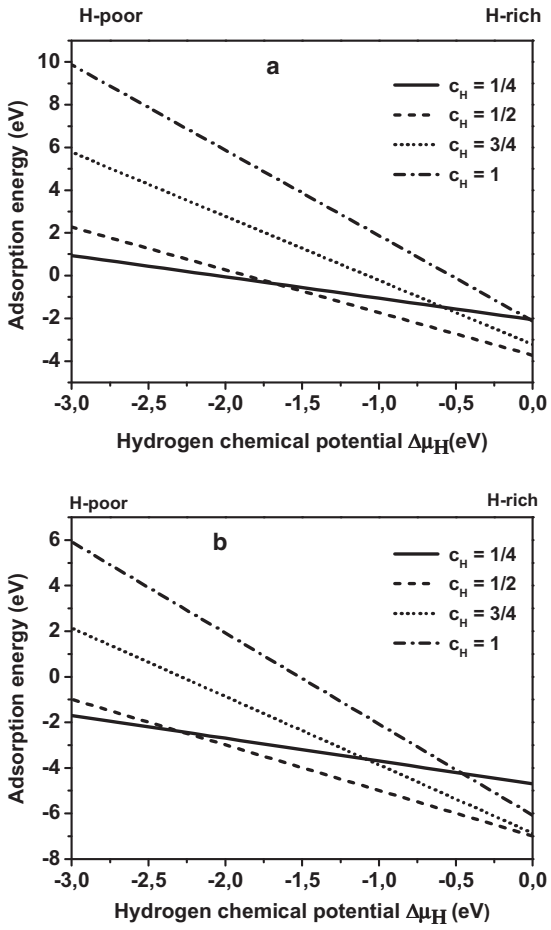

Fig. 2. The calculated GGA–PBE adsorption energy vs. hydrogen chemical potential as obtained for: a) clean and b) Mg-doped ZnO $\left(000\bar{1}\right)$ surface respectively.

the two quantities. The surface energy specifies the energy change per surface area and is related to the average adsorbed H formation energy through the simple relation [37]:

$$nE_a = \Delta\gamma \times A(surface\ \ Area) \tag{8}$$

where n is the number of adsorbed H atoms.

On the other hand, the obtained results show that the adsorbed atomic hydrogen is energetically more stable on the Mg-doped ZnO $\left(000\bar{1}\right)$ surface than the undoped surface and this is true for all possible hydrogen coverage conditions. This means that the Mg-doped ZnO and wurtzite $Mg_xZn_{1-x}O$ surfaces are much efficient for atomic hydrogen adsorption or hydrogen detection than the clean O-terminated ZnO surface. Experimental studies show that Mg doping of ZnO nanowires increases the hydrogen storage capacity [38]. On the other side, ZnO thin films doped with Mg atom exhibit hydrogen sensing characteristic better than the undoped films [39]. These results appear to be in good agreement with our results. On the other hand, we have calculated the adsorption energy for atomic hydrogen on the Mg-doped ZnO $\left(000\bar{1}\right)$ surface for both O-rich and O-poor growth conditions (Fig. 3). The obtained results show that the hydrogen adsorption is much favored onto Mg-doped surface prepared under O-rich growth conditions. These results are very important for constructing hydrogen storage devices or hydrogen gas sensors.

Now we turn our attention to the electronic properties of the investigated surfaces. The calculated density of states (DOS) for undoped ZnO $\left(000\bar{1}\right)$ surface under different H coverage conditions are showed in

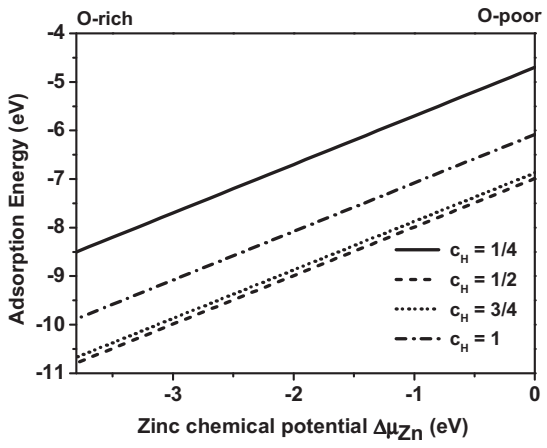

Fig. 3. The calculated GGA–PBE adsorption energy vs. zinc chemical potential for Mg-doped ZnO $\left(000\bar{1}\right)$ surface under different H coverage conditions.

Fig. 4. The clean ZnO $\left(000\bar{1}\right)$ surface shows semiconducting properties with the presence of empty surface state levels in the gap. These states are the results of the top surface O dangling bonds which give rise to partially occupied O-2p-band. Adsorbing 1/4 ML of hydrogen on the surface oxygen atoms decreases the surface states DOS located near the top of the valence band without changing the semiconducting properties of the ZnO $\left(000\bar{1}\right)$ surface (Fig. 4b). In this case, an electron is transferred from the adsorbed H atom to the surface but this is not sufficient to fill completely the O-2p-band (partial passivation). Adsorbing 1/2 ML of hydrogen removes completely the surface states

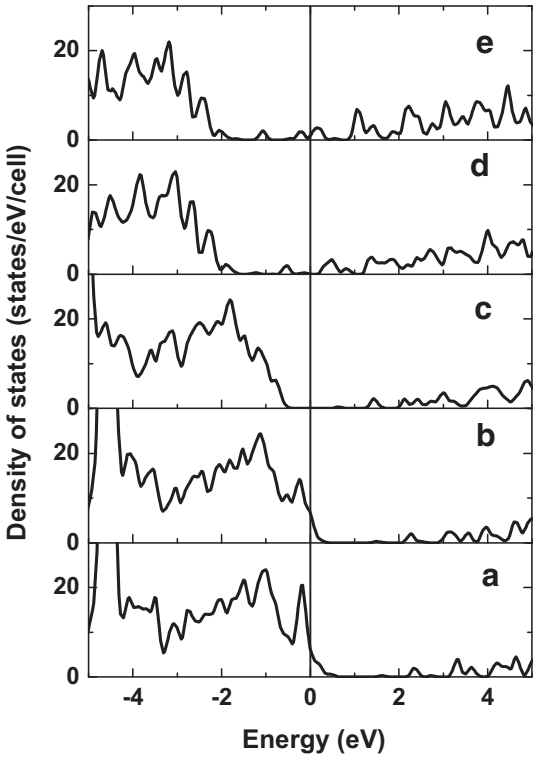

Fig. 4. The calculated density of states (DOS) for ZnO $\left(000\bar{1}\right)$ surface under different H coverage conditions, a) clean surface, b) 1/4 ML H adsorbed, c) 1/2 ML H adsorbed, d) 3/4 ML H adsorbed, and e) 1 ML H adsorbed. The vertical line shows the Fermi energy position.

from the band gap and produces a semiconducting surface with a direct gap of 1.25 eV. Adsorbing more hydrogen on the O surface (3/4 ML and 1 ML) induces metallicity with bands crossing the Fermi level. Since each adsorbed H atom provides one electron to the ZnO surface, starting from 1/2 ML two electrons will fill the partially occupied O-2P band and the excess of electrons will partially occupy the 4 s of the surface Zn atoms (the conduction band). The obtained surface in this case is *n* type (metallic behavior). This is different from the case of $\left(1\bar{1}00\right)$ surface where H adsorption coverage of 1/4 ML is sufficient to transform the surface to conducting state [40].

The Mg doping of the ZnO $\left(000\bar{1}\right)$ surface doesn't change the previous concluding remarks and this is because Mg atom is an isoelectronic dopant and can form with ZnO a ternary alloy $Mg_xZn_{1-x}O$. In the previous work, Bai et al. [16] show that the doping of ZnO with donor such as Al atom enhances the gas sensing characteristics of this material. Based on our results we can suggest the existence of two mechanisms to do this, first mechanism can be done by donor atom doping and the second is based on isoelectronic atom doping like Mg and perhaps Be atoms. On the other hand, the Mg doping of the surface affects considerably the H_2 adsorption energy. The calculated adsorption energies for molecular hydrogen are −0.15 eV and −3.1 eV for both undoped and Mg-doped ZnO $\left(000\bar{1}\right)$ surfaces respectively. This means that the H_2 adsorption is more favored on Mg-doped than onto the undoped structure.

Now we will discuss the effect of H adsorption on the structural properties of undoped and Mg-doped ZnO $\left(000\bar{1}\right)$ surfaces. For this purpose we calculate the average percent change from bulk for the first three interlayer spacings called *d1*, *d2* and *d3* respectively as defined in Fig. 5. The obtained results are listed in Table 2. These results suggest a strong response of the top interlayer spacing to hydrogen adsorption for both undoped and Mg-doped surfaces. For the hydrogen-free undoped surface, *d1* is contracted 48.3% from the bulk, while the fully covered surface results in a 19% expansion. These values are in good agreement with the previous results of Chamberlin et al. [41] who find values of −50% and +25% for hydrogen-free and fully covered surface respectively. The layers below *d1* are also affected by hydrogen adsorption and their responses depend greatly on the amount of adsorbed hydrogen. In the case of Mg-doped surface the relaxation is more important and this is related to the small size of Mg atom compared to zinc atom. For the hydrogen-free Mg-doped surface the obtained results show that the first layer *d1* is contracted more than the undoped case.

Now we turn our attention to the optical properties of the investigated surfaces. The imaginary part $\varepsilon_2(\omega)$ of the dielectric function $\varepsilon(\omega)$ is calculated from the momentum matrix elements between the occupied and unoccupied electronic states using first order time-dependent perturbation theory. The real part $\varepsilon_1(\omega)$ of the dielectric function $\varepsilon(\omega)$ is evaluated from the imaginary part $\varepsilon_2(\omega)$ by the Kramers–Kronig transformation. The absorption coefficient $\alpha(\omega)$ and reflectivity $R(\omega)$ can be obtained from $\varepsilon_1(\omega)$ and $\varepsilon_2(\omega)$ using the following expressions;

$$\alpha(\omega) = \sqrt{2}\omega\left[\sqrt{\varepsilon_1(\omega)^2 + \varepsilon_2(\omega)^2} - \varepsilon_1(\omega)\right]^{1/2} \quad (9)$$

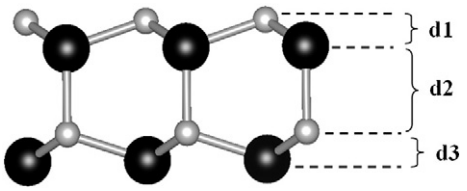

Fig. 5. The first three interlayers *d1*, *d2* and *d3* of the ZnO $\left(000\bar{1}\right)$ polar surface. Oxygen and zinc atoms are represented by small grey and large black spheres respectively.

Table 2
Average percent change from bulk for the first three interlayer spacing as obtained in this work for both undoped and Mg-doped for 0, 1/4, 1/2, 3/4 and 1 ML hydrogen covered surfaces.

Layer	Clean surface			Mg-doped surface		
	% Δ*d*1	% Δ*d*2	% Δ*d*3	% Δ*d*1	% Δ*d*2	% Δ*d*3
0 ML	−48.37%	+3.10%	−12.44%	−50.77%	+2.49%	−14.56%
1/4 ML	−25.22%	+1.73%	−6.00%	−26.42%	+1.18%	−6.16%
1/2 ML	−1.34%	−0.07%	+2.02%	−5.32%	−0.56%	+1.09%
3/4 ML	+11.23%	−1.77%	+4.97%	+9.59%	−2.30%	+8.77%
1 ML	+19.28%	−1.98%	+8.24%	+15.13%	−2.08%	+12.46%

$$R(\omega) = \left|\frac{1-\sqrt{\varepsilon(\omega)}}{1+\varepsilon(\omega)}\right|^2. \quad (10)$$

This approach is implemented in several DFT codes and it is widely used to study the optical properties of materials [42–44].

To study the effect of atomic hydrogen adsorption on the optical properties of the ZnO surface we have calculated the optical reflectivity spectra for both undoped and Mg-doped ZnO $\left(000\bar{1}\right)$ surfaces under different hydrogen coverage conditions and the obtained results are illustrated in Fig. 6. Our results show that Mg doping of the ZnO surface can lead to an increase in the optical reflectivity of this surface in the photon energy range of 0–0.5 eV while it decreases in the 1.2–2.5 eV range. H atom adsorptions induce a large change in the optical reflectivity spectra of the ZnO surface. These changes were found to be depending on the H coverage. Compared to the clean surface case, a decrease of the surface optical reflectivity in the photon energy range of 0–0.6 eV was showed for all H coverages. The H adsorption coverage of 1/2 monolayer makes the surface more transparent to IR photon and this is due to the passivation of all surface states by the tow H atoms leading to an increase in the surface gap. For high H coverage conditions ($c_H > 1/2$), the surface will exhibit a nearly 100% optical reflectivity peak located in the range of 1.0–1.5 eV.

Fig. 7 shows the optical absorption spectra as obtained by our calculations for Mg-doped O-terminated ZnO surface under different H coverage conditions. It is very clear that the optical absorption coefficient of the surface depends greatly on the adsorbed H amount. For clean surface, the optical absorption spectra show the presence of three peaks in the [0–1 eV] range which are attributed to many optical transitions such as; i) direct optical transition from valence band (VB) to the conduction band (CB), ii) direct optical transition between surface states and CB. For low H adsorption coverage ($c_H = 1/4$), the number of optical absorption peaks in the [0–1 eV] range was reduced

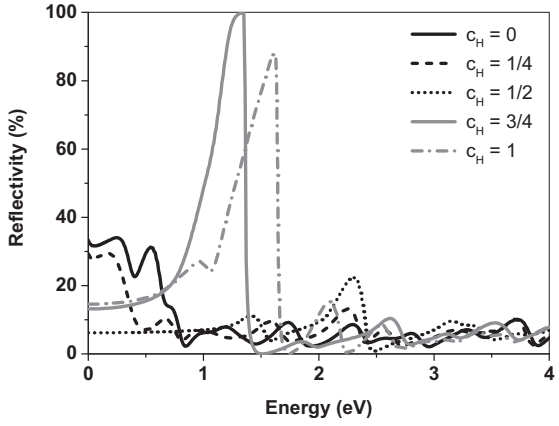

Fig. 6. The optical reflectivity spectra of the Mg-doped ZnO $\left(000\bar{1}\right)$ surface under different hydrogen coverages.

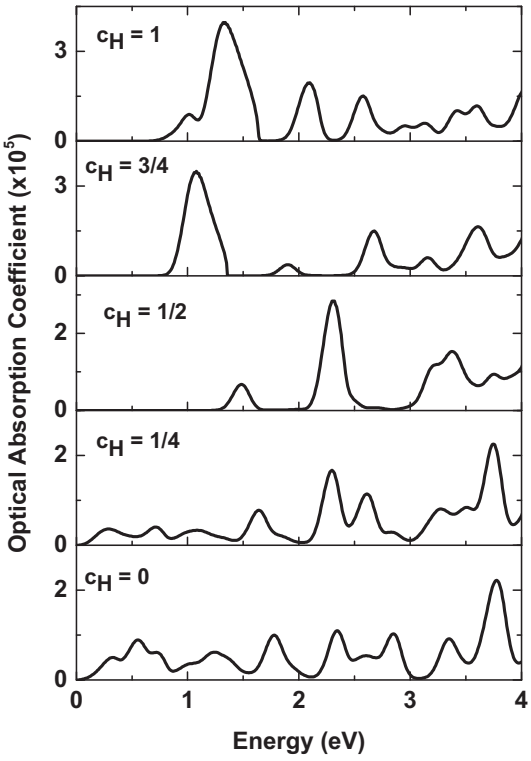

Fig. 7. The optical absorption coefficient of the Mg-doped ZnO $\left(000\bar{1}\right)$ surface under different hydrogen coverages.

and this is due to the partial passivation of surface states by atomic hydrogen adsorption. For $c_H = 1/2$ monolayer the optical absorption coefficient spectra show no peaks in the [0–1 eV] range and this is due to the full passivation of surface states by adsorbed atomic hydrogen. It is very known that up to 1/2 monolayer of hydrogen we fill the partially occupied O-2p-band, beyond the 1/2 monolayer the O-2p-band is completely filled and we have to populate the conduction band. These make the optical properties of the surface very sensitive to the H coverage conditions.

4. Conclusions

In this work, the effect of hydrogen adsorption on the properties of both clean and Mg-doped ZnO $\left(000\bar{1}\right)$ polar surface was investigated using the first principles method. The obtained results show that hydrogen adsorption is energetically more favored on Mg-doped ZnO $\left(000\bar{1}\right)$ surface than the clean surface. Our results show also that the hydrogen adsorption on the Mg doped surface is energetically more favored if the surface was grown under O-rich conditions than O-poor conditions. We have also examined the effect of H adsorption on the optical properties of the Mg-doped ZnO $\left(000\bar{1}\right)$ surface. The obtained results show that the optical properties of the Mg-doped ZnO $\left(000\bar{1}\right)$ surface are very sensitive to the hydrogen coverage conditions.

References

[1] C. Klingshirn, Phys. Status Solidi B 244 (2007) 3027.
[2] Ü. Özgür, Ya.I. Alivov, C. Liu, A. Teke, M.A. Reshchikov, S. Doğan, V. Avrutin, S.-J. Cho, H. Morkoç, J. Appl. Phys. 98 (2005) 041301.
[3] D. Scarano, S. Bertarione, G. Spoto, A. Zecchina, C. Otero Areán, Thin Solid Films 400 (2001) 50.
[4] A. Wander, N.M. Harrison, J. Phys. Chem. B 105 (2001) 6191.
[5] J.B. Lopes Martins, E. Longo, O.D. Rodríguez Salmon, V.A.A. Espinoza, C.A. Taft, Chem. Phys. Lett. 400 (2004) 481.
[6] R. Lindsay, E. Michelangeli, B.G. Daniels, T.V. Ashworth, A.J. Limb, G. Thornton, A. Gutièrrez-Sosa, A. Baraldi, R. Larciprete, S. Lizzit, J. Am. Chem. Soc. 124 (2002) 7117.
[7] M. Kunat, U. Burghaus, Ch. W ll, Phys. Chem. Chem. Phys. 5 (2003) 4962.
[8] J.B.L. Martins, C.A. Taft, S.K. Lie, E. Longo, J. Mol. Struct. (Thoechem) 528 (2000) 161.
[9] J. Yu, M. Shafiei, M. Breedon, K. Kalantar-zadeh, W. Wlodarski, Procedia Chemistry 1 (2009) 979.
[10] O. Melikhova, et al., J. Alloy Comp. 580 (2013) S40.
[11] X. Lu, X. Xu, N. Wang, Q. Zhang, J. Phys. Chem. B 103 (1999) 2689.
[12] B. Meyer, Phys. Rev. B 69 (2004) 045416.
[13] M. Casarin, C. Maccato, A. Vittadini, Inorg. Chem. 37 (1998) 5482.
[14] Rizwan Wahab, Farheen Khan, Naushad Ahmad, Hyung-Shik Shin, Javed Musarrat, A. Abdulaziz, Al-Khedhairy, J. Nanomater. (2013) 542753.
[15] A.B. Usseinov, E.A. Kotomin, A.T. Akilbekov, Y.F. Zhukovskii, J. Purans, Phys. Scr. 89 (2014) 045801.
[16] S. Bai, T. Guo, Y. Zhao, R. Luo, D. Li, A. Chen, C.C. Liu, J. Mater. Chem. A. 1 (2013) 11335.
[17] H. Xu, W. Fan, A.L. Rosa, R.Q. Zhang, Th. Frauenheim, Phys. Rev. B 79 (2009) 073402.
[18] A. Calzolari, A. Catellani, J. Phys. Chem. C 113 (2009) 2896.
[19] A. Wander, N.M. Harrison, J. Chem. Phys. 115 (2001) 2312.
[20] J. Beheshtian, A.A. Peyghan, Z. Bagheri, Appl. Surf. Sci. 258 (2012) 8171.
[21] C. Wongchoosuk, S. Choopun, A. Tuantranont, T. Kerdcharoen, Mater. Res. Innov. 13 (2009) 185.
[22] J.S. Wright, W. Lim, D.P. Norton, S.J. Pearton, F. Ren, J.L. Johnson, A. Ural, Semicond. Sci. Technol. 25 (2010) 024002.
[23] Y. Gai-Yu, D. Kai-Ning, L. Jun-Qian, Chinese J. Struct. Chem. 29 (2010) 1139.
[24] Q. Yuan, Ya-Pu. Zhao, L. Li, T. Wang, J. Phys. Chem. C 113 (2009) 6107.
[25] J.D. Prades, A. Cirera, J.R. Morante, Sensors Actuators B 142 (2009) 179.
[26] Cong-sheng Tian, Xin-liang Chen, J. Ni, Jie-ming Liu, De-kun Zhang, Q. Huang, Y. Zhao, Xiao-dan Zhang, Sol. Energy Mater. Sol. Cells 125 (2014) 59.
[27] A. Agrawal, T. Ahmad Dar, P. Sen, J. Nano Electron. Phys. 5 (2013) 02025.
[28] Q. Xu, Xiu-Wen Zhang, Wei-Jun Fan, Shu-Shen Li, Shu-Shen Li, Shu-Shen Xia, Comput. Mater. Sci. 44 (2008) 72.
[29] J. Bang, H. Yang, P.H. Holloway, Nanotechnology 17 (2006) 973.
[30] D. Sánchez-Portal, P. Ordejón, E. Artacho, J.M. Soler, Int. J. Quantum Chem. 65 (1997) 453.
[31] J.M. Soler, E. Artacho, J.D. Gale, A. Garca, J. Junquera, P. Ordejón, D. Sánchez-Portal, J. Phys. Condens. Matter 14 (2002) 2745.
[32] N. Troullier, J.L. Martins, Phys. Rev. B 43 (1991) 1993.
[33] J.P. Perdew, A. Zunger, Phys. Rev. B 23 (1981) 5048.
[34] J.P. Perdew, K. Burke, M. Ernzerhof, Phys. Rev. Lett. 77 (1996) 3865.
[35] E. Badaeva, Y. Feng, D.R. Gamelin, X. Li, New J. Phys. 10 (2008) 055013.
[36] Z. Yufei, G. Zhiyou, G. Xiaoqi, C. Dongxing, D. Yunxiao, Z. Hongtao, J. Semicond. 31 (2010) 082001.
[37] G. Kresse, O. Dulub, U. Diebold, Phys. Rev. B 68 (2003) 245409.
[38] H. Pan, J. Luo, H. Sun, Y. Feng, C. Poh, J. Lin, Nanotechnology 17 (2006) 2963.
[39] Y. Liu, T. Hang, Y. Xie, Z. Bao, J. Song, H. Zhang, E. Xie, Sensors Actuators B 160 (2011) 266.
[40] A.B. Usseinov, E.A. Kotomin, A.T. Akilbekov, Y.F. Zhukovskii, J. Purans, Thin Solid Films 553 (2014) 38.
[41] S.E. Chamberlin, C.J. Hirschmugl, S.T. King, H.C. Poon, D.K. Saldin, Phys. Rev. B 84 (2011) 075437.
[42] J. Hu, B.C. Pan, J. Appl. Phys. 105 (2009) 083710.
[43] R.M. Sheetz, I. Ponomareva, E. Richter, A.N. Andriotis, M. Menon, Phys. Rev. B 80 (2009) 195314.
[44] L. Guan, B. Liu, Q. Li, Y. Zhou, J. Guo, G. Jia, Q. Zhao, Y. Wang, G. Fu, Phys. Lett. A 375 (2011) 939.